

Superfluids under High Speed Rotation

example: $^3\text{He-A}$: Anisotropic Superfluid
studied by NMR line width change

Minoru Kubota

Institute for Solid State Physics, Univ. Tokyo

For a simple superfluid, example $^4\text{He II}$,

$$\Omega_{c1}: \quad \Omega_{c1} = h \ln(R/a) / (2\pi m_4 R^2)$$

R: vessel radius

$$\Omega_{c2}: \quad \Omega_{c2} = h / 2\pi m_4 a^2.$$

a: vortex core diameter

but, ...in ^3He ... a little bit more of things.

Rotating DR Cryostats in the world

TABLE I

Characteristics of Rotating mK Cryostats. The columns refer to: (i) the appropriate reference; (ii) the year when the cryostat started operating; (iii) the mode in which the dilution refrigerator is operated in rotation [1-Shot Single Cycle or Continuous Recycling]; (iv) how the pumping of the cryostat is organized in rotation [with Rotating Vacuum Seals or by Means of one or Several Alternating Cryo-Adsorption Pumps (cp)]; (v) type of bearings used to support the rotation of the cryostat [1×Oil—One Horizontal Pressurized Oil Bearing, 3×Air—One Horizontal Support Bearing and Two Vertical Stabilizing Bearings, Air Pads—Individually Adjusted Air Pads, Usually 3 for Horizontal Support and 3 For Vertical Stabilization, 2×Air—One Compact Horizontal and One Vertical Air Bearing]; (vi) location of the analog electronics [Rotating with the Cryostat, in a Separate Synchronously Rotating Cradle, or Connected via a Multiple-Slip-Ring Assembly]; (vii) maximum rotation velocity.

Cryostat	Ref.	Start year	Dil. ref.	Pumping	Bearings	Analog instr.	Max Ω (rad/s)
Berkeley I	11	1973	cont	rot seals	air pads	rotating	1
Cornell	12	1979	cont	rot seals	1 × oil	rotating	0.5
Helsinki I	13	1981	1-shot	1 × cp	3 × air	rotating	4
Helsinki II	14	1988	cont	4 × alt cp	3 × air	synch	6
Berkeley II	15	1990	cont	rot seals	air pads	slip ring	4
Manchester I	16	1990	cont	rot seals	air pads	rotating	2
Manchester II	17	1992	cont	rot seals	air pads	rotating	4
Tokyo I	18	1994	cont	rot seals	2 × air	synch	7
Tokyo II	18	2001	cont	rot seals	2 × air	synch	25

->38

R. Blaauwgeers, S. Boldarev, V. B. Eltsov, A. P. Finne, and M. Krusius

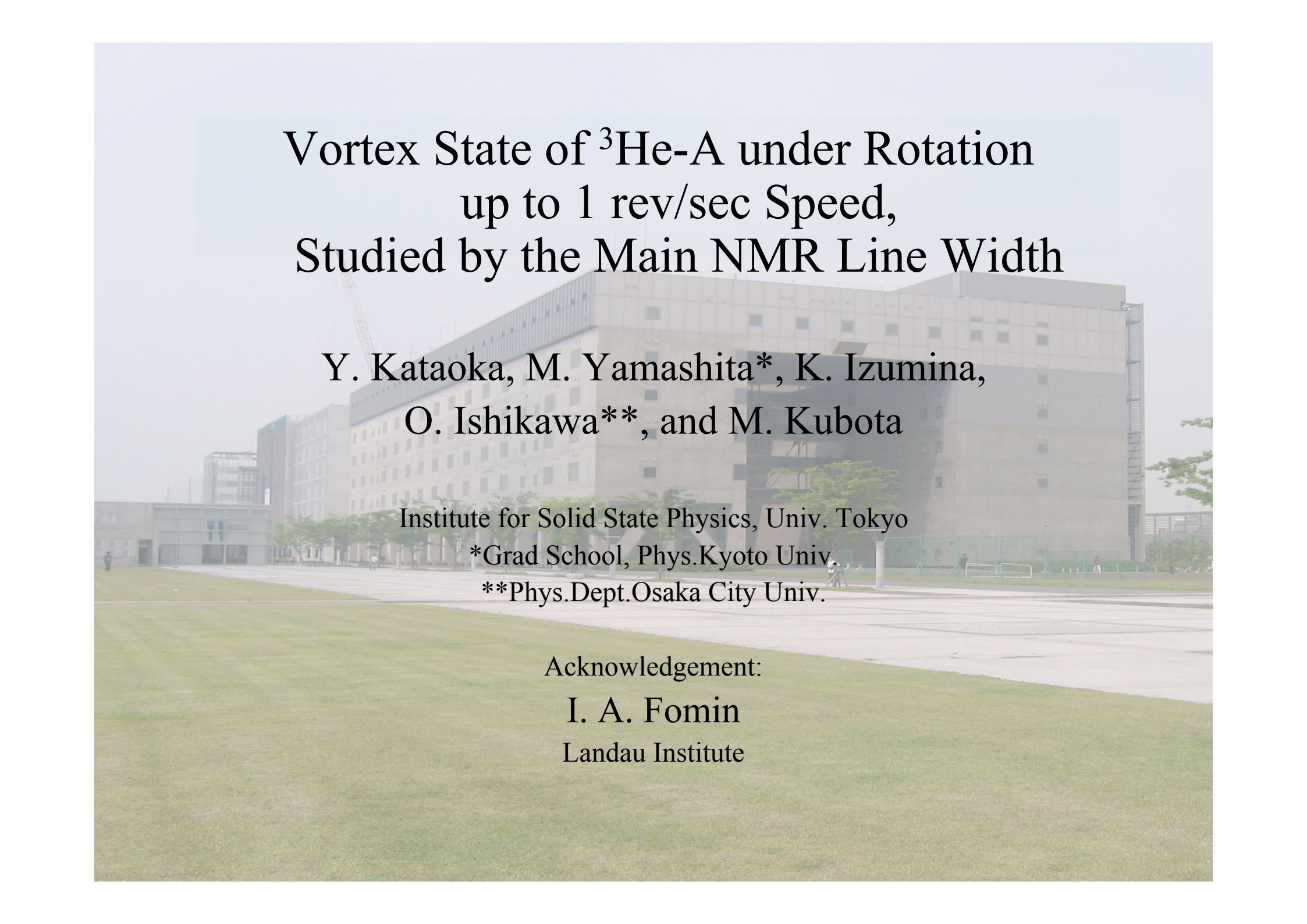
Journal of Low Temperature Physics, Vol. 132, Nos. 5/6, September 2003 (© 2003)

When we discussed desired experimental conditions in 2000, we had finished the ground design of ISSP ULT Rota, cooperators expressed their wish to have
 $< 3\text{rad/sec}$

As you may have seen in the previous talk, for all of our work, 6.28 rad/sec maximum rotational speed has been essential for the results.

Then: Is it possible further to increase the rotational speed Ω ?
Are there many interesting phenomena for experimental study at such increased Ω ?

This is Kubota group's own activity to pursue this direction and I will show you one of such subjects below.



Vortex State of $^3\text{He-A}$ under Rotation
up to 1 rev/sec Speed,
Studied by the Main NMR Line Width

Y. Kataoka, M. Yamashita*, K. Izumina,
O. Ishikawa**, and M. Kubota

Institute for Solid State Physics, Univ. Tokyo

*Grad School, Phys. Kyoto Univ.

**Phys. Dept. Osaka City Univ.

Acknowledgement:

I. A. Fomin

Landau Institute

NMR study of $^3\text{He-A}$ under rotation

Satelites and main NMR signal change have been studied under rotation :

As to Main NMR Peak change:

Early Helsinki study by NMR as well as recent one at a constant temperature.

We report on the main line width change as a function of temperature as well as rotational speed to up to 1 revolution /sec.

We have observed three distinct regions with correct τ dependences, as described by Fomin and Kaminskii(1982), for the first time .

We have confirmed linear Ω dependence in $\Delta\Gamma$ near T_c , as to the lower temperature Ω dependence, we observe something different from the above scenario. Non-linear effect is clear.

NMR study of $^3\text{He-A}$ under rotation (So far reported relevant results).

1]. P.J. Hakonen, et. al., PRL Vol.48, 1838 (1982), "NMR Experiments on Rotating Superfluid $^3\text{He-A}$: Evidence for Vorticity"

2]. P.J. Hakonen, O.T. Ikkala, S.T. Islander, Phys. Rev. Lett. Vol.49,1258 (1982). "Experiments on Vortices in Rotating Superfluid $^3\text{He-A}$ ".

3]. I.A. Fomin and V.G. Kamenskii, JETP Lett. Vol.35, 302 (1982), "Effect of Rotation on the NMR signal in the Helium-3 A Phase".

4]. P.J. Hakonen, et. al., J.Low Temp. Phys. Vol.53, 425 (1983), "NMR Experiments on Rotating Superfluid $^3\text{He-A}$ and $^3\text{He-B}$ and Their Theoretical Interpretation".

5]. P.J. Hakonen, M.Krusius, and H.K. Seppaelae, J. Low Temp. Phys.Vol.60, 187 (1985), "NMR Studies on Vortices in Rotating $^3\text{He-A}$ ".

6]. Ue. Parts, J.M. Karimaeki, J.H. Koivuniemi, M. Krusius, V. M.H. Ruutu, E.V. Thuneberg, and G.E. Volovik, Phys. Rev. Lett.Vol.75, 3320 (1995), "Phase Diagram of Vortices in Superfluid $^3\text{He-A}$ ".

7]. V.B. Eltsov, R. Blaauwgeers, M. Krusius, J.J. Ruohio, and R. Schanen, J. Low Temp. Phys.Vol.124, 123 (2001), "NMR Spectroscopy of the Double-Quantum Vortex in Superfluid $^3\text{He-A}$ ".

P.J. Hakonen, M.Krusius, and H.K. Seppaelae, J. Low Temp. Phys. Vol.60, 187 (1985), "NMR Studies on Vortices in Rotating $^3\text{He-A}$ ".

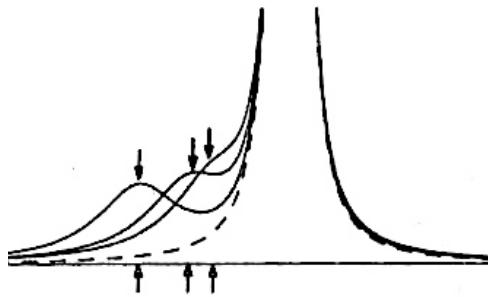


Fig. 9. Locations of the satellite maxima (upper arrows) as compared to the center frequencies of Lorentzian satellites (lower arrows) close to a Lorentzian main peak.

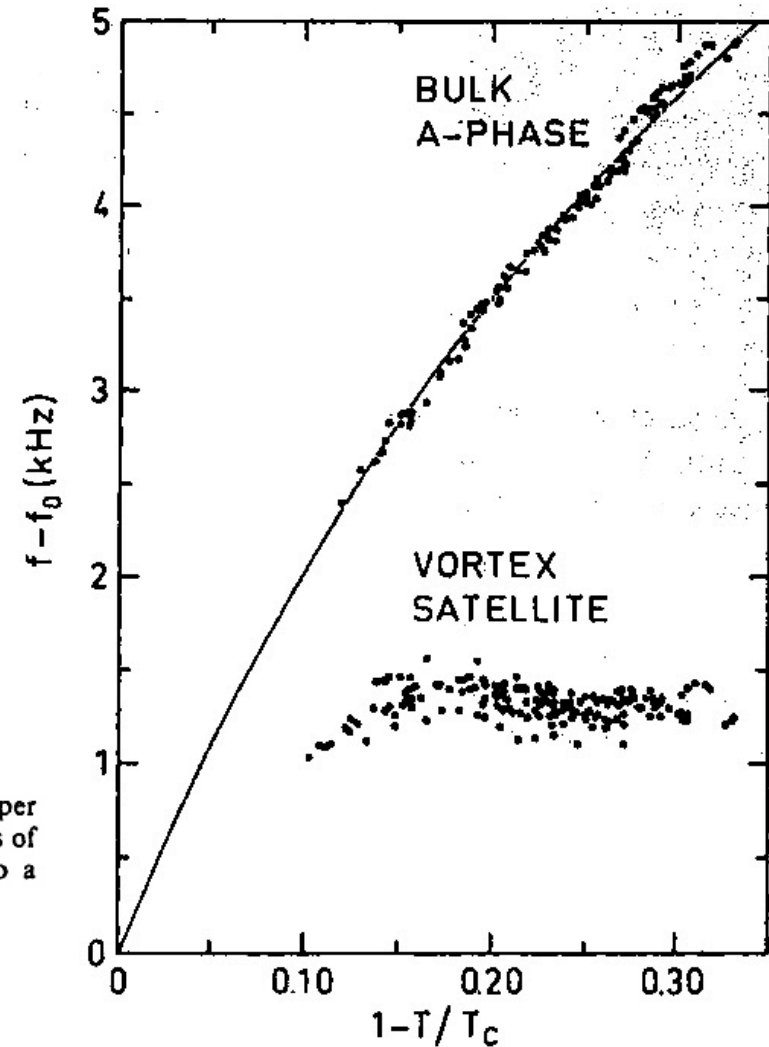
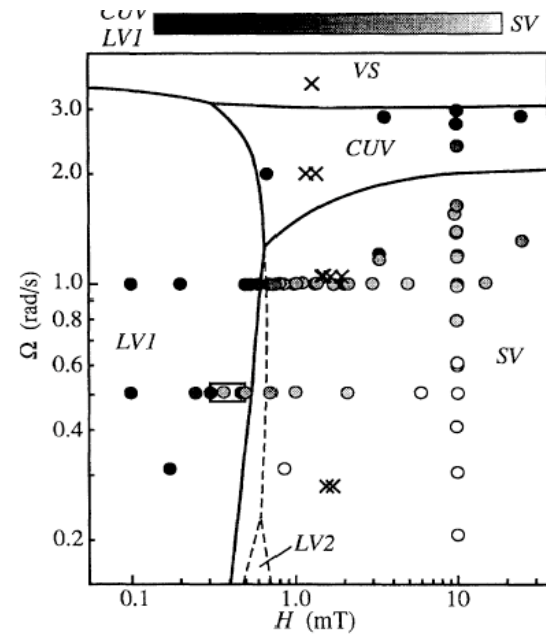
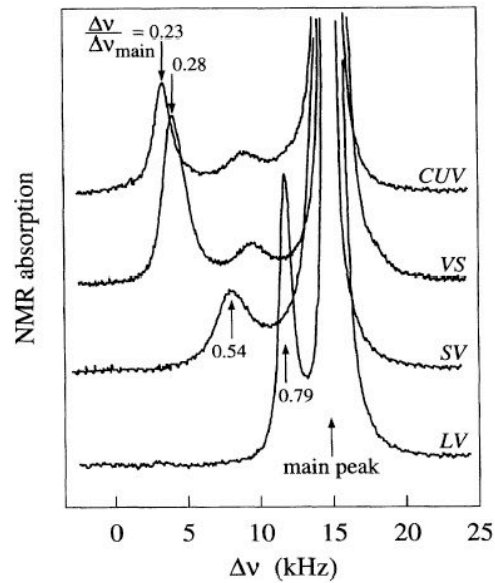
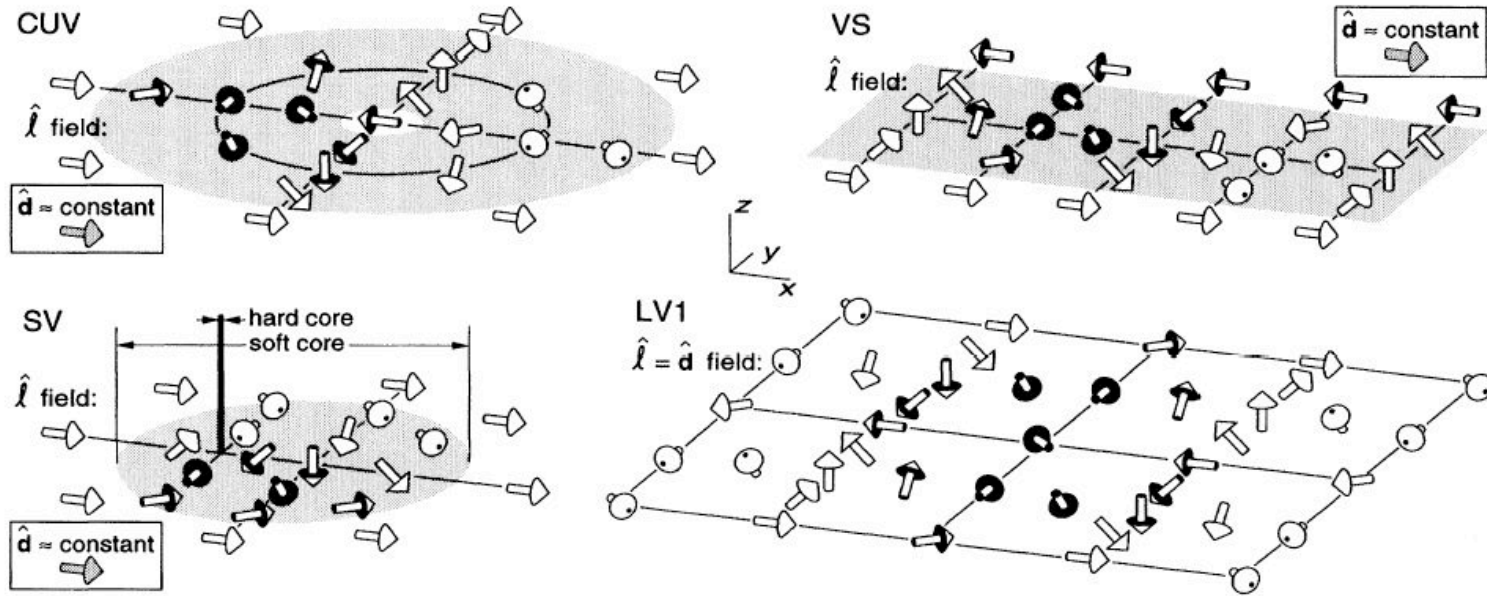


Fig. 10. The frequency shift of the vortex satellite $f_v - f_0$ as a function of temperature $1 - T/T_c$ from various experiments at $\Omega = 0.6-1.4$ rad/sec and $B = 28.4$ mT. The bulk A-phase shift $f_A - f_0$ is also displayed.

Parts, et.al. Phys. Rev. Lett. Vol.75, 3320 (1995).
 "Phase Diagram of Vortices in Superfluid $^3\text{He-A}$ "



V.B.Eltsov, R.Blaauwgeers, M.Krusius, J.J.Ruohio and R.Schanen ,
NMR Spectroscopy of the Double-Quantum Vortex in Superfluid 3He-A,
Journal of Low Temperature Physics, Vol.124, 123 (2001).

CUV: continuously unlocked vortex

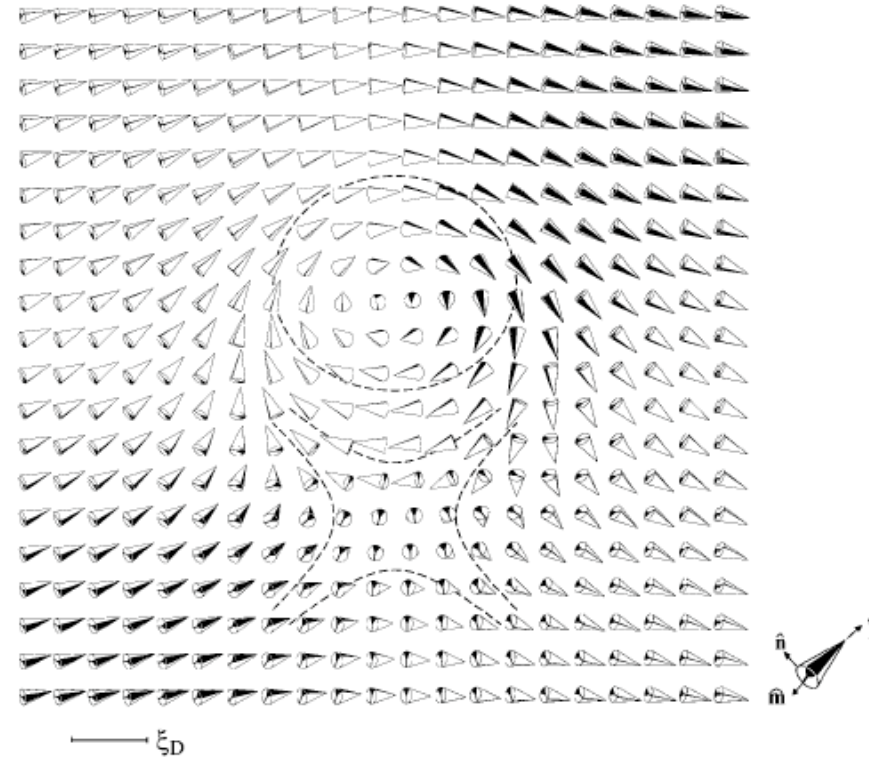


Fig. 1. Orbital order parameter field in the soft core of the double-quantum vortex. In the order parameter $A_{\mu\nu} = \Delta_0 \hat{\mathbf{d}}_\mu (\hat{\mathbf{m}}_\nu + i\hat{\mathbf{n}}_\nu)$, the amplitude Δ_0 is constant across the core and also the orientation of the spin anisotropy axis $\hat{\mathbf{d}}$ is almost constant. The continuous distributions of $\hat{\mathbf{m}}$, $\hat{\mathbf{n}}$, and $\hat{\mathbf{l}} = \hat{\mathbf{m}} \times \hat{\mathbf{n}}$ are shown. The rotation of $\hat{\mathbf{m}}$ and $\hat{\mathbf{n}}$ around $\hat{\mathbf{l}}$ plays the role of the order parameter phase and can be seen to wind by 4π along a path far way around the core. Thus this vortex carries two quanta of circulation. The vortex is not axially symmetric and the two Mermin-Ho vortices or merons with circular and hyperbolic winding of $\hat{\mathbf{l}}$ are clearly separated. The length scale for the structure is the healing length of the spin-orbit interaction ξ_D .

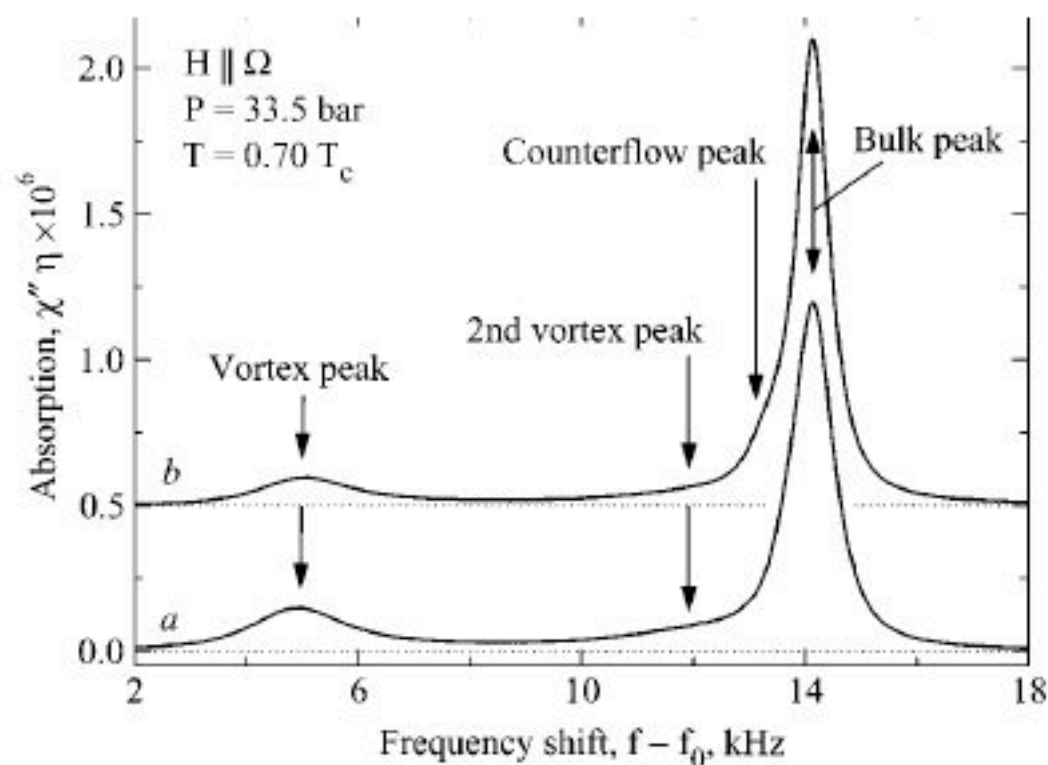


Fig. 2. NMR spectra of rotating $^3\text{He-A}$ with double-quantum vortex lines. (a) Spectrum measured during decelerating rotation at the annihilation threshold ($\Omega = 2.5 \text{ rad/s}$). It consists of the large bulk-liquid peak and two vortex satellites: The ground-state satellite is well resolved at small frequency shift, while the excited state is responsible for the broad shoulder closer to the bulk peak. (b) Spectrum measured during accelerating rotation at the critical velocity threshold ($\Omega = 1.8 \text{ rad/s}$). In addition to the bulk and vortex satellite peaks, on the left flank of the former the absorption from the vortex-free counterflow region is visible.

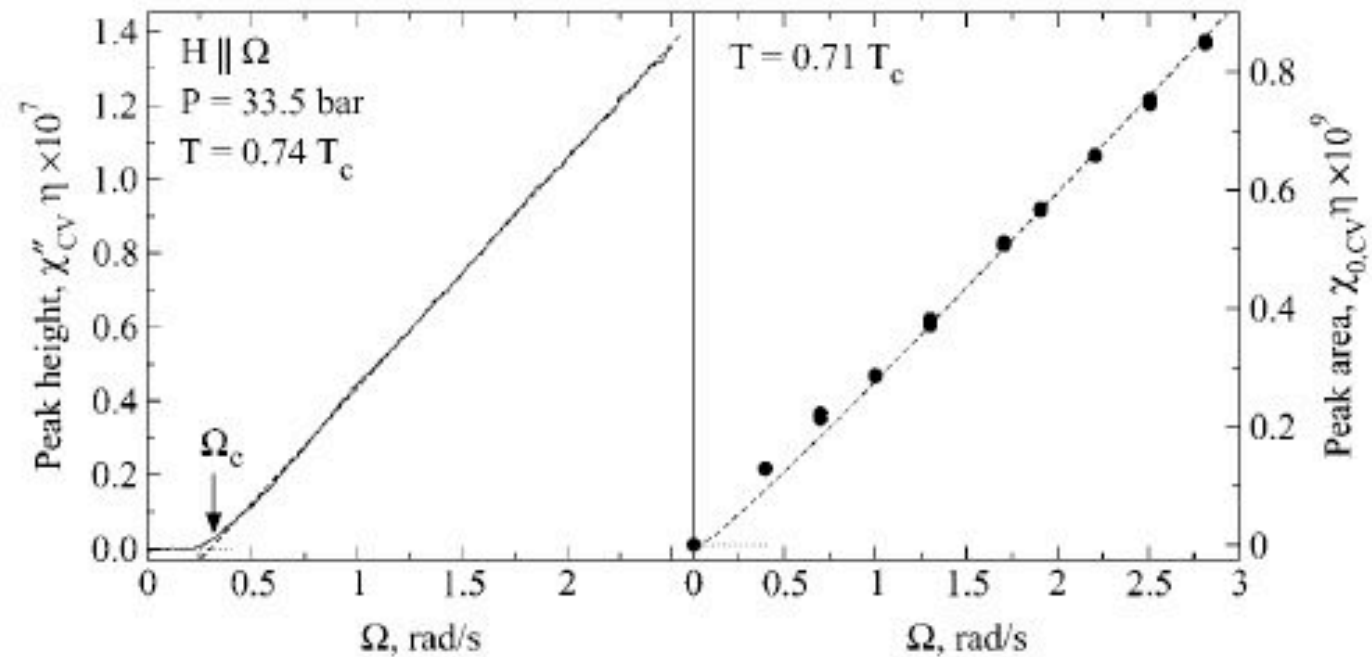


Fig. 3. Vortex-satellite absorption during increasing and decreasing rotation: (Left) Peak height A of satellite as a function of Ω during accelerating rotation. Beyond the critical rotation velocity $\Omega_c = 0.32$ rad/s the absorption is proportional to the number of vortex lines in Eq. (1). The dashed straight line is a linear fit $A = A_0 (\Omega - \Omega_c)$. (Right) Integrated satellite absorption I during decelerating rotation, when the vortex cluster is at the annihilation threshold. The absorption is again proportional to the number of vortices, in this case given by Eq. (2). The dashed line is a fit $I = I_0 (\Omega - \sqrt{\Omega^* \Omega})$, where $\Omega^* = 0.041$ rad/s is from Ref. 11, but scaled to the radius of the present sample container.

Experimental Conditions

Pressure: $P=30.5$ bar

Cylinder diameter: 3.0mm

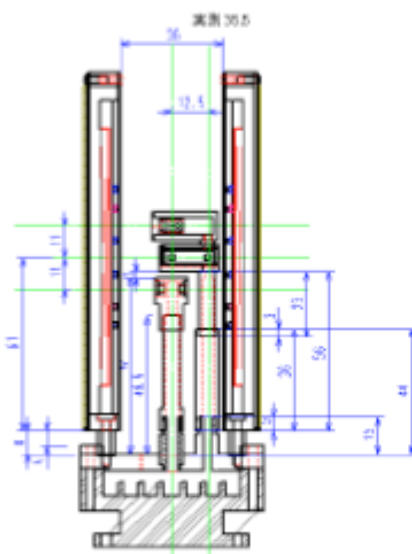
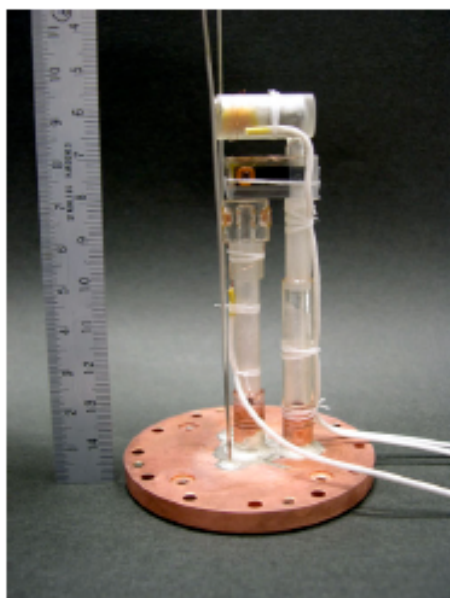
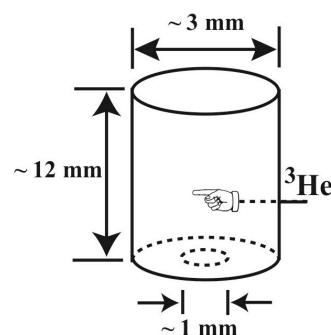
NMR frequency : 700 kHz

Rotational angular velocity:

$\Omega -6.28 - 0 - +6.28$ rad/sec.

Temperature:

We scan both temperature and rotational angular velocity.



NMR signal under stil conditions

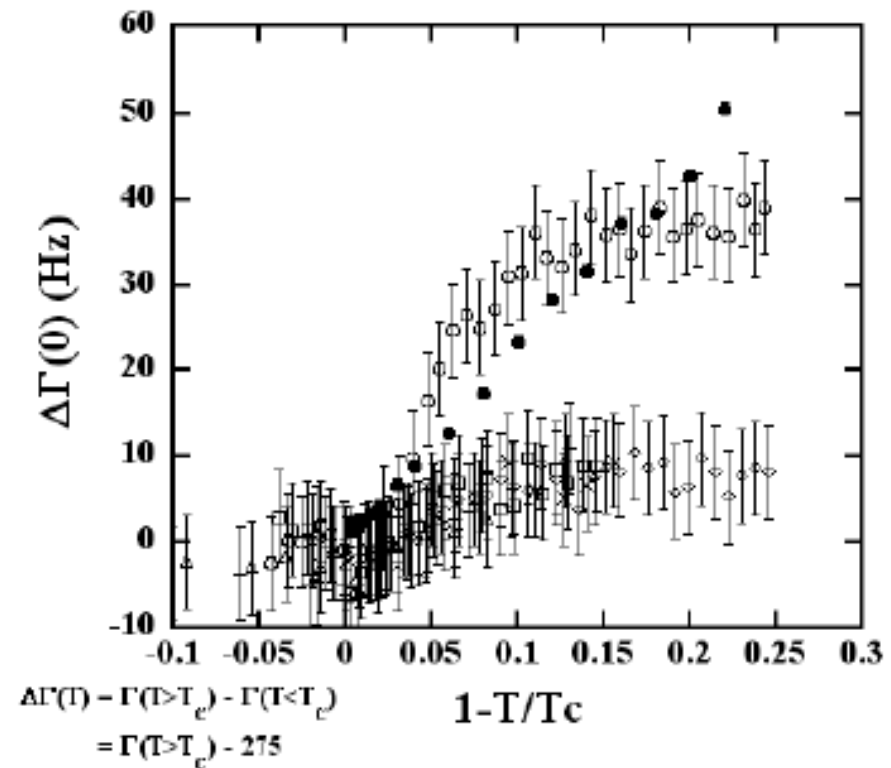


図 6.16 静止下の温度変化による線幅の増加

縦軸は線幅の増加 $\Delta\Gamma(0)$ ，横軸は換算温度 $1 - \frac{T}{T_c}$ である。
線幅とは半値幅のことである。

各測定点は、

(○) 冷却過程 2004.6.10-12, (□) 加熱過程 2004.6.10-12,

(◇) 冷却過程 2004.10.8-11, (×) 加熱過程 2004.10.8-11,

(+) 冷却過程 2004.10.4-5, (△) 加熱過程 2004.10.4-5,

(●) 融解圧力下における Gully et al. (1976) の縦共鳴の測定結果^[34]
を横共鳴の値に換算した頁 34 の図 2.11 の値を引用したものに
対応している。

Fomin and Kamenskii (1982)'s discussion on bulk $^3\text{He-A}$ main NMR peak line width $\Delta\Gamma$

In addition to the vortex peak, which grows in proportion to Ω ,
There should be effect caused by fluctuations to the main NMR line.
Namely, the line width change $\Delta\Gamma$ should have such dependences:
As to Ω dependence, they supposed linear dependence.

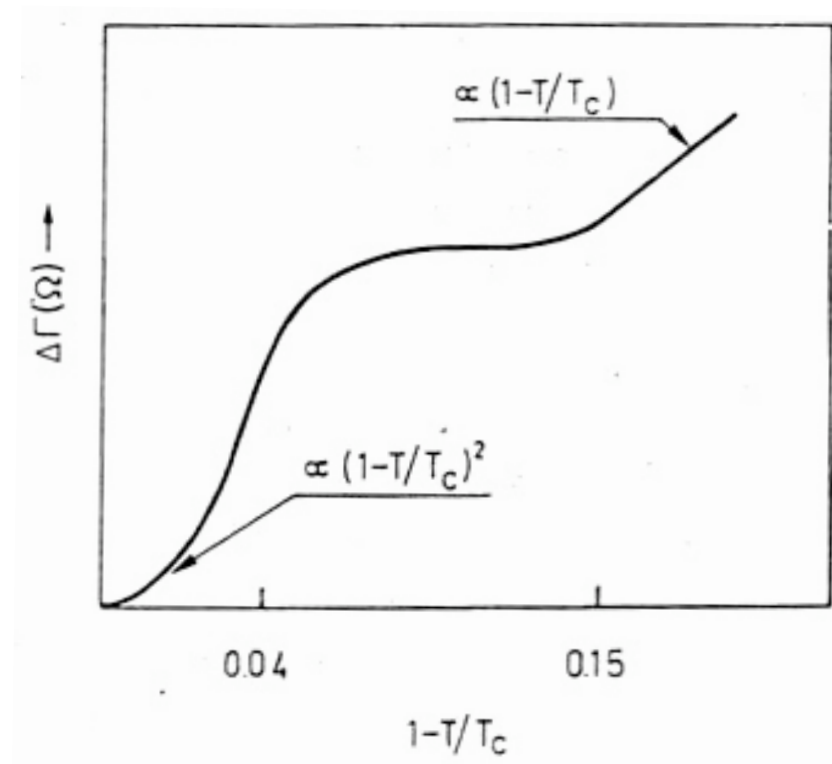
1]. $T \sim T_c$ ($\tau = 1 - T/T_c < 0.04$)

Spin diffusion is most important: $\Delta\Gamma \sim \alpha\tau^2$

2]. $0.06 < \tau < 0.12$

Plateau in $\Delta\Gamma$ should appear

3]. $\tau > 0.2$: $\Delta\Gamma \sim \beta\tau$



Experimental work on bulk $^3\text{He-A}$ main peak line width under rotation:

P.J. Hakonen,
M.Krusius, and H.K.
Seppaelae, J. Low
Temp. Phys.Vol.60,
187 (1985), "NMR
Studies on Vortices
in Rotating $^3\text{He-A}$ "

They observed plateau in the
 $\Delta\Gamma$ as a function of reduced
Temperature, $\tau = 1-T/T_c$, but not
any n for τ^n .

V.B. Eltsov, R. Blaauwgeers, M. Krusius, J.J. Ruohio, and R. Schanen,
JLTP, vol. 124, 123 (2001).

Ω sweep at a constant
temperature, $0.7T_c$.

$$\Delta\Gamma \sim \Omega^{3/2}$$

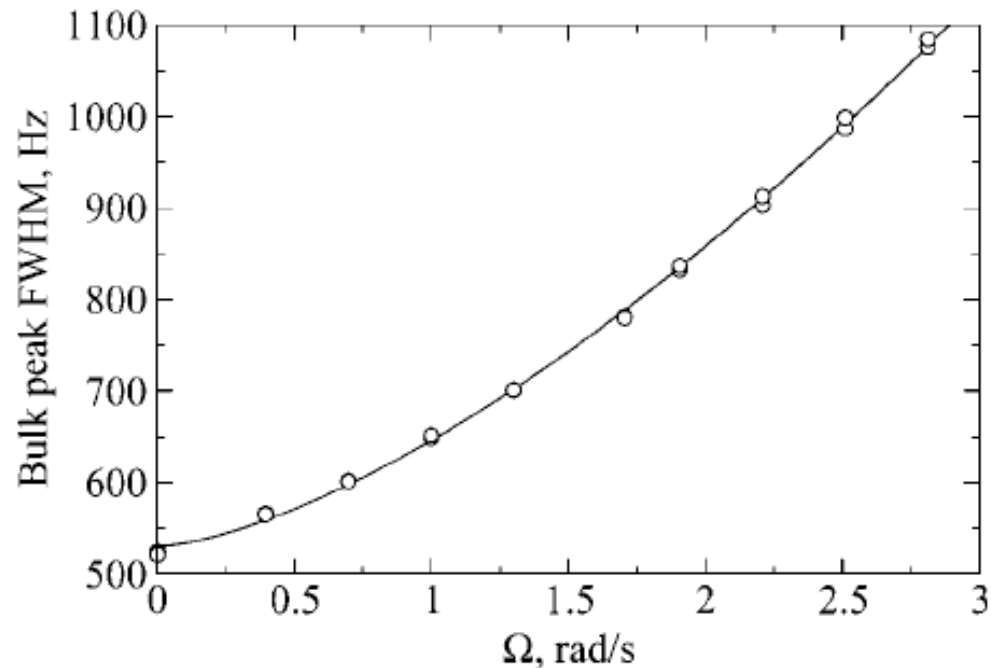
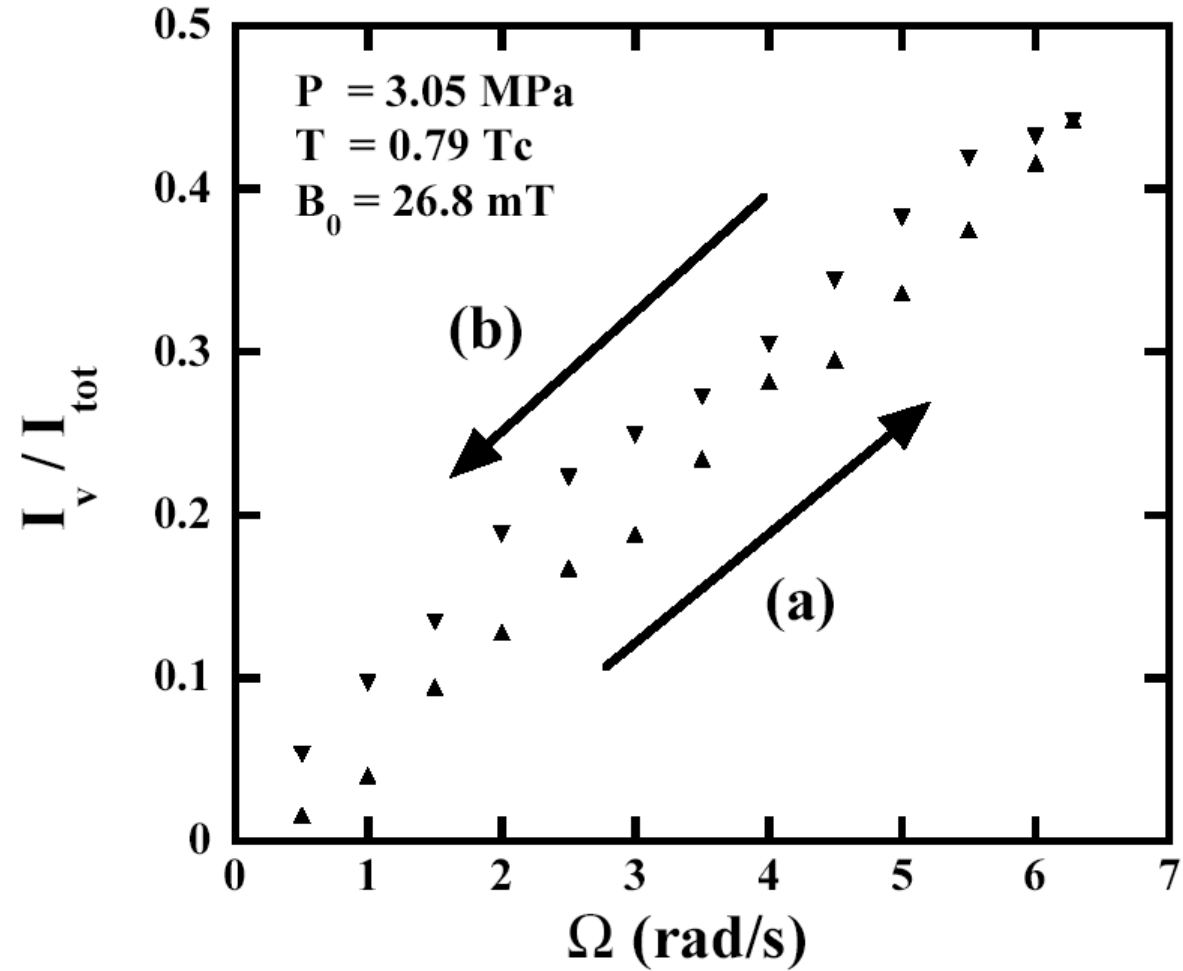


Fig. 16. Line width of the bulk-liquid peak, expressed as full width at half maximum. The width has been measured at the annihilation threshold as a function of rotation velocity, i.e. the number of double-quantum vortex lines corresponds closely to equilibrium. The solid line is a fit to the data: $\Gamma = 530 + 116\Omega^{3/2}$ (with Γ in Hz and Ω in rad/s). In the normal phase the width is $\Gamma = 140$ Hz.

CUV or Vortex Sheet(VS) ?

0].



Our measurements

0]. $\Delta I/I$ vs τ

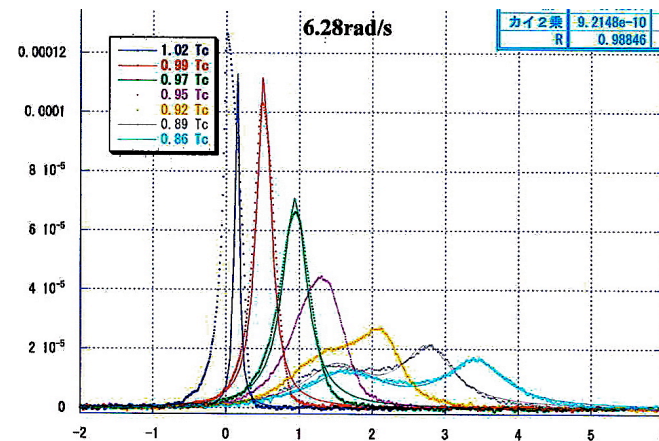
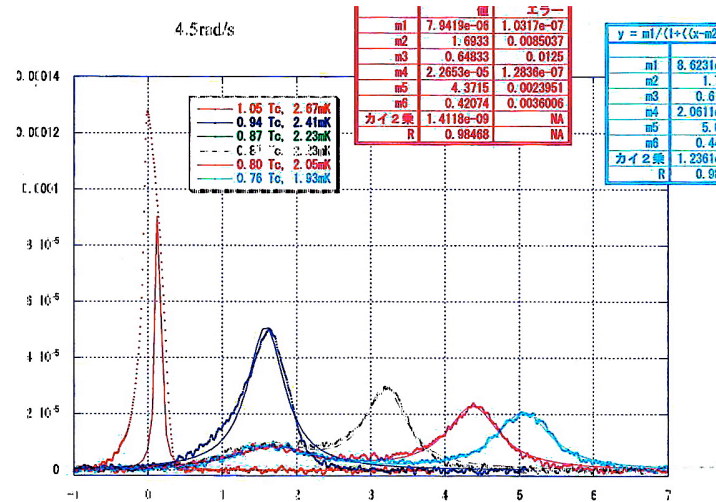
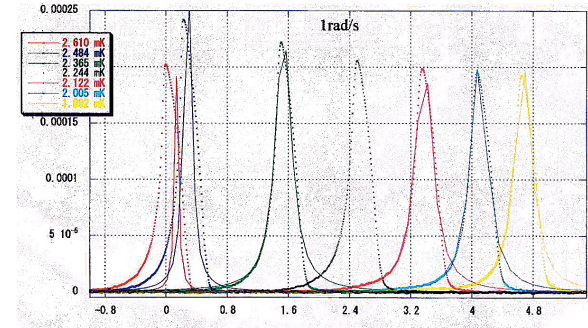
1]. Temperature sweeps at constant Ω 's.

And

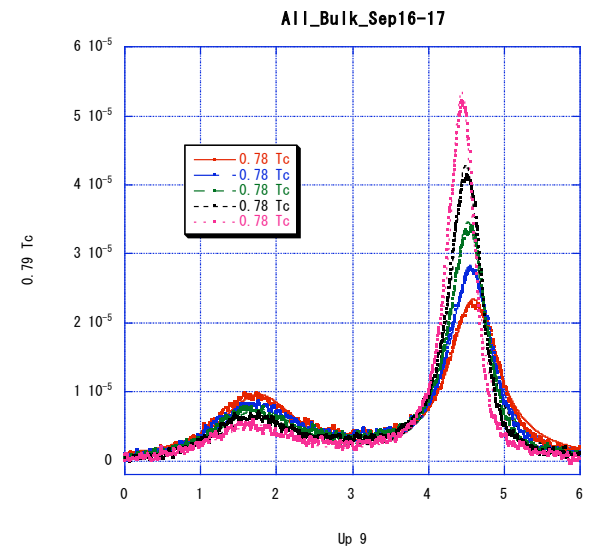
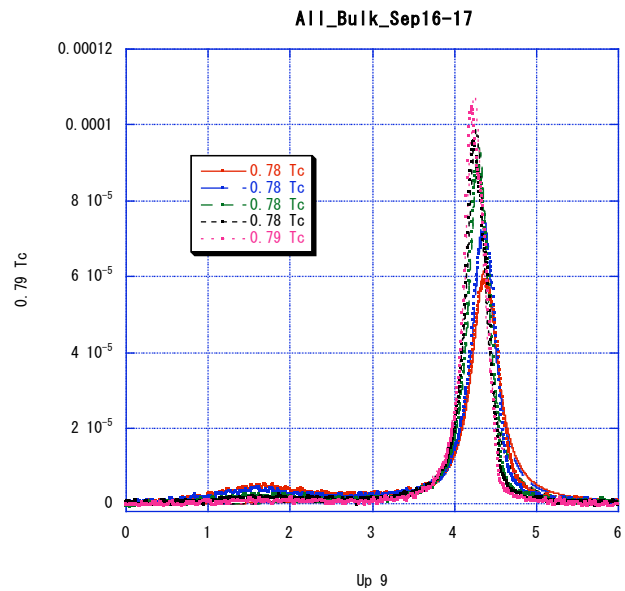
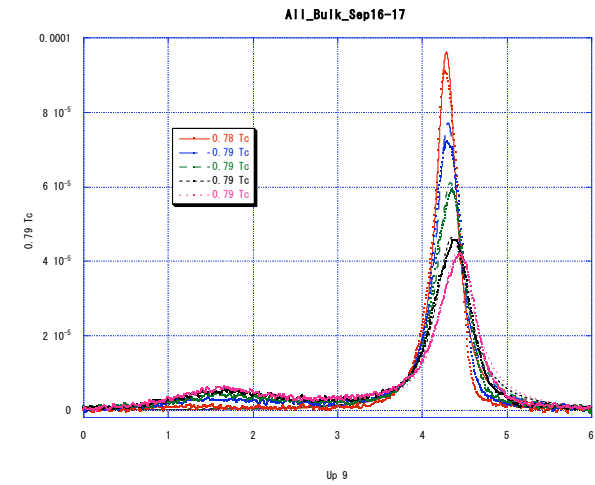
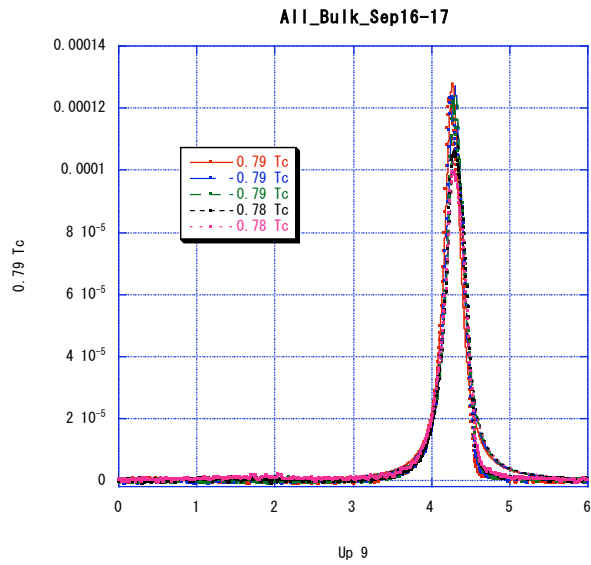
2]. Ω sweeps at constant temperatures (next page)

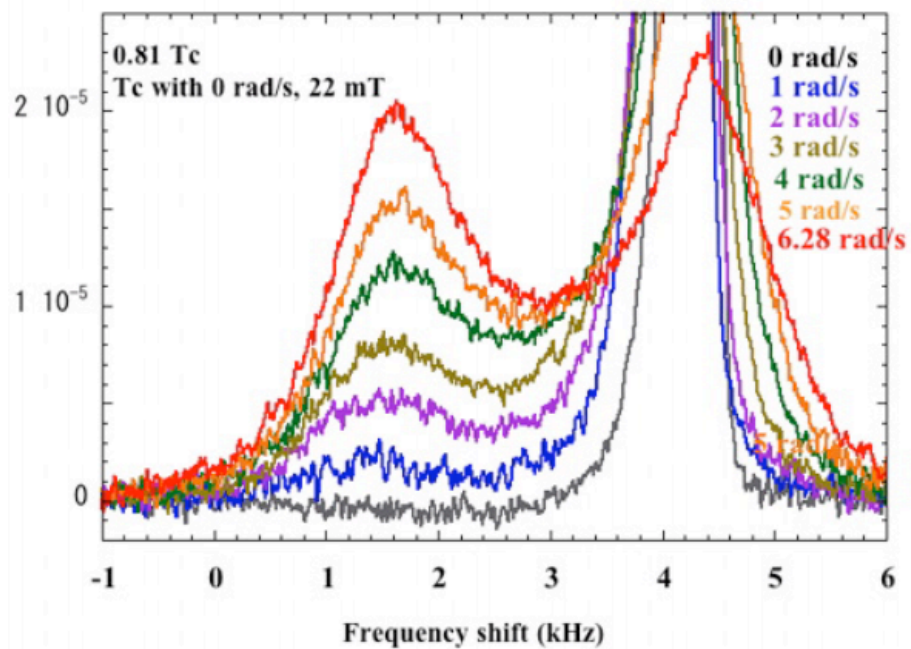
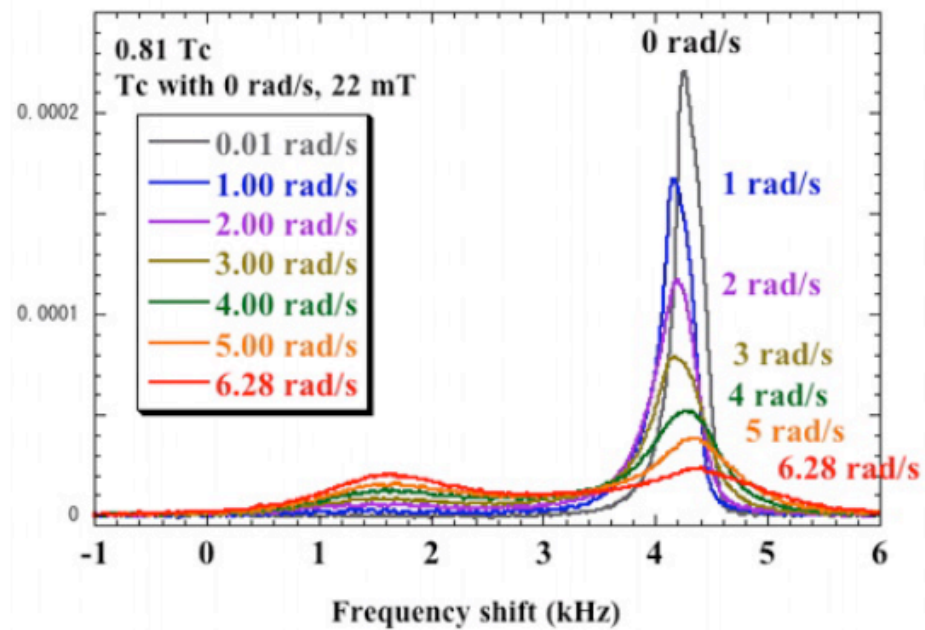
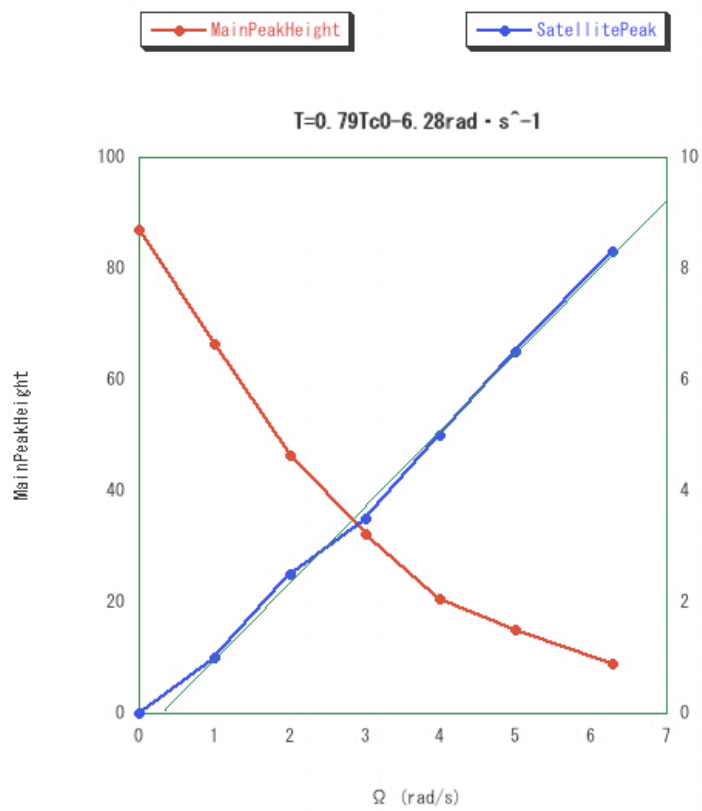
Have been performed.

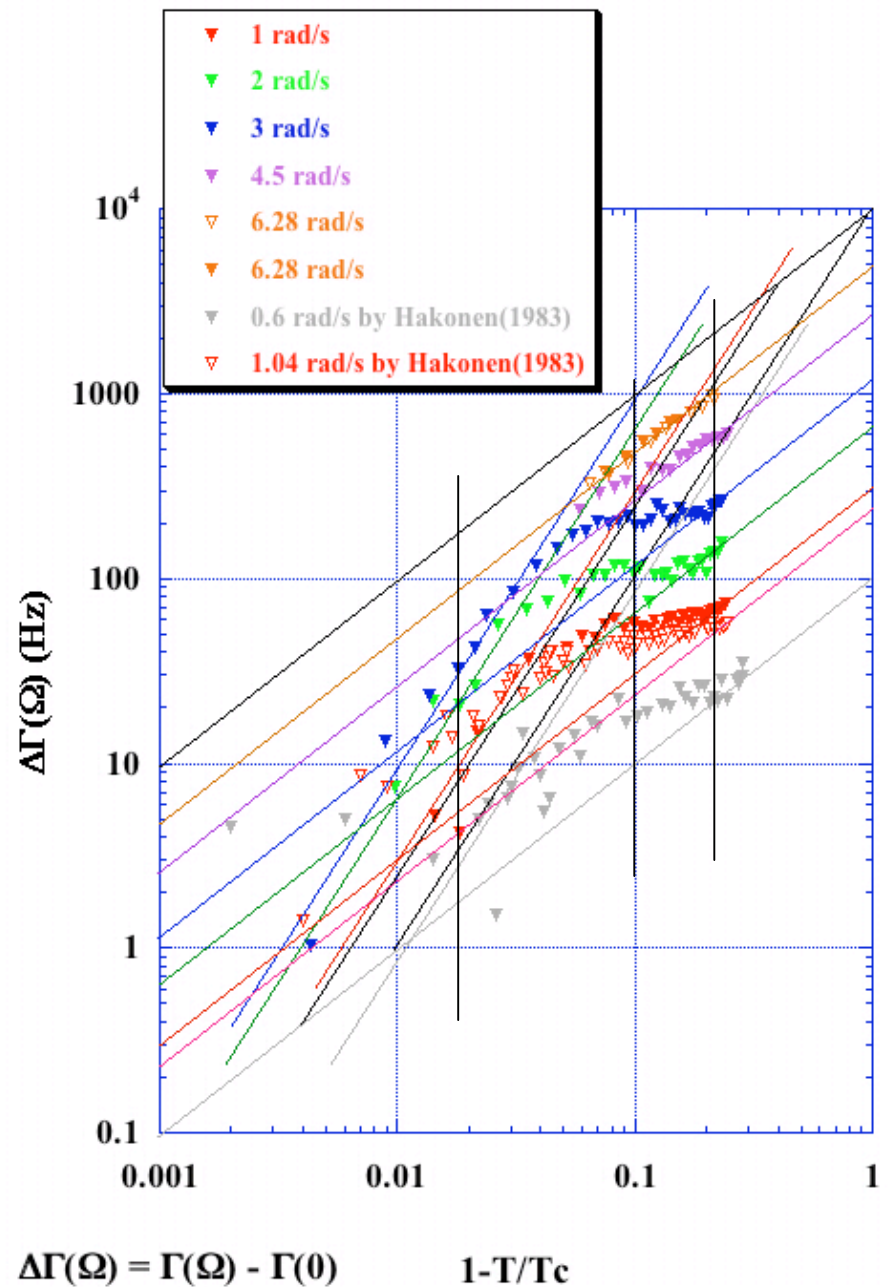
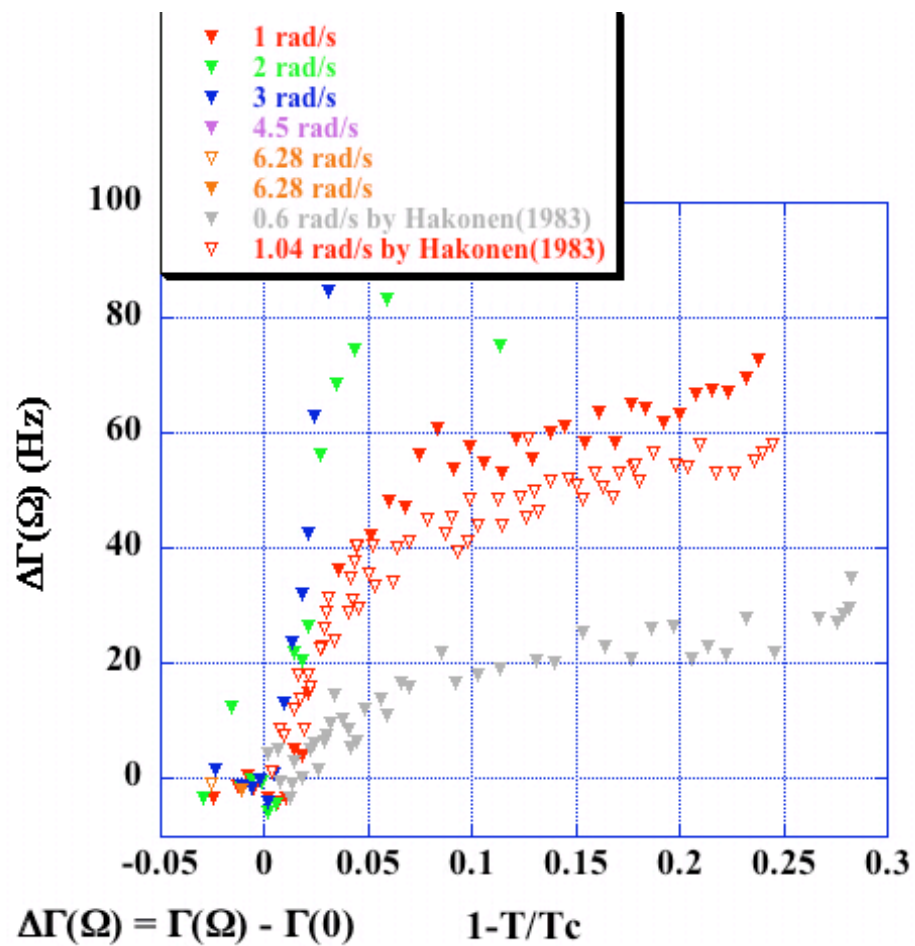
1].



2]. Ω sweep at constant temperature $\sim 0.8T_c$



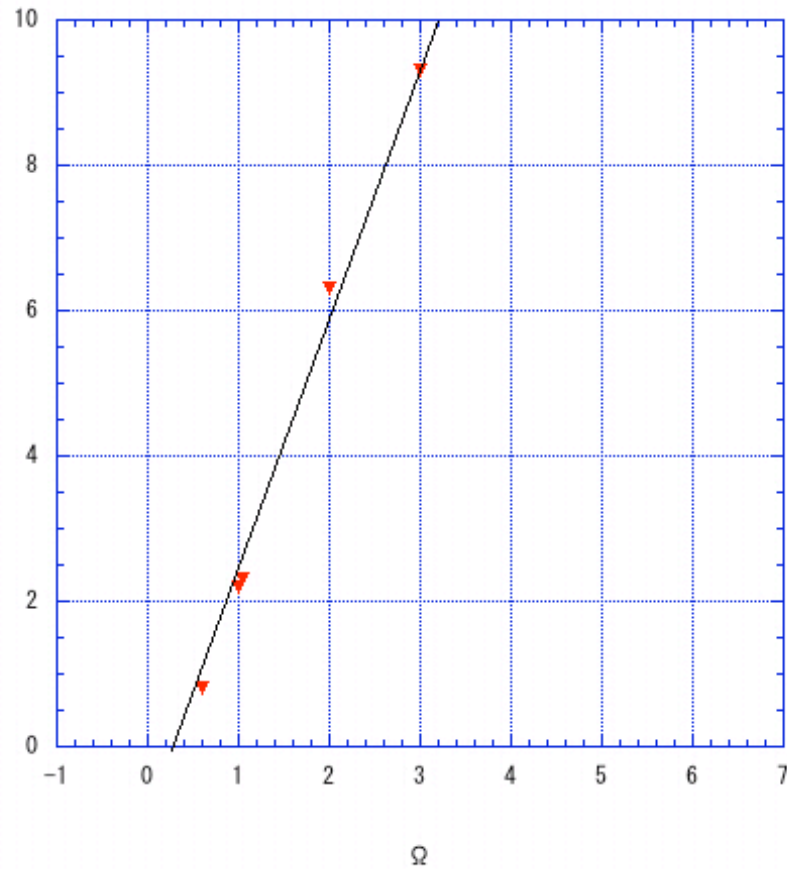




τ -linear, τ^2 parameters as Ω , Ω^2

▼ B

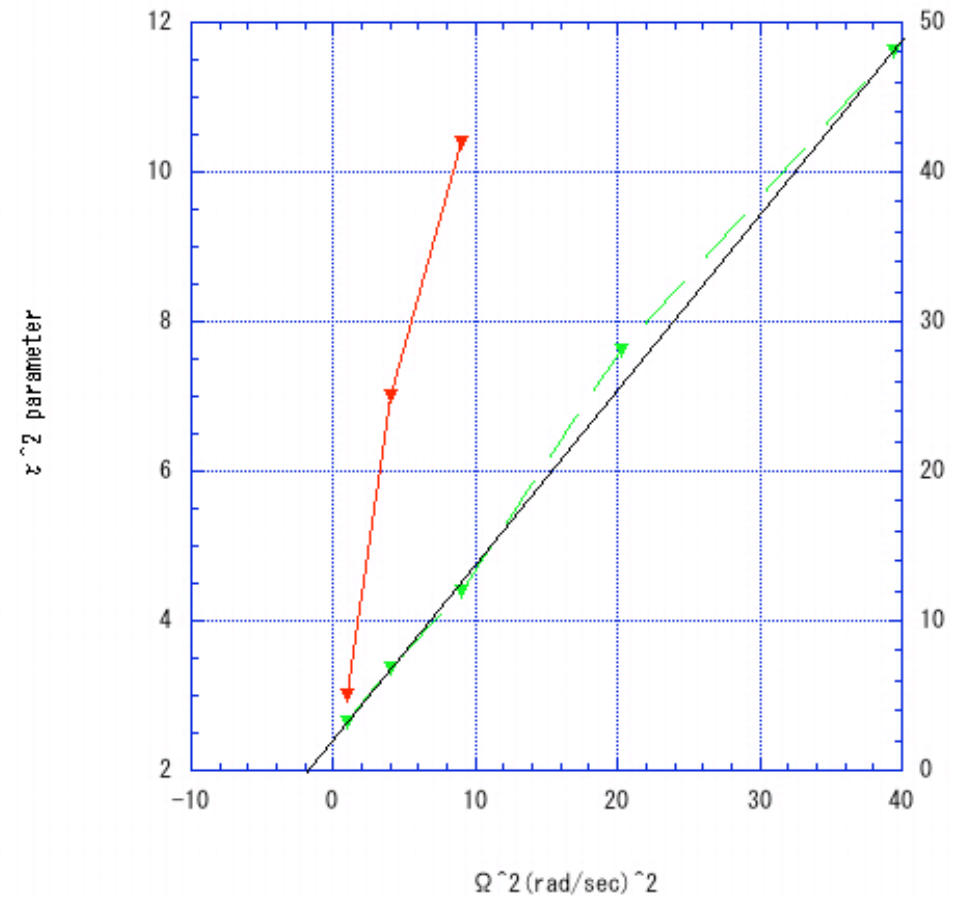
HakonenKata τ^2 係数

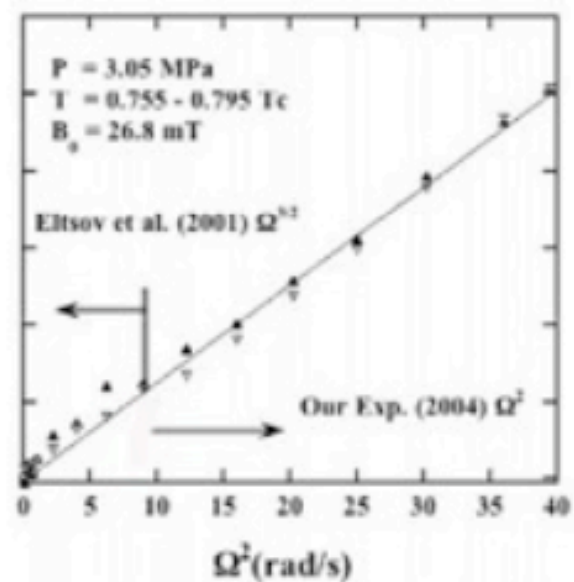
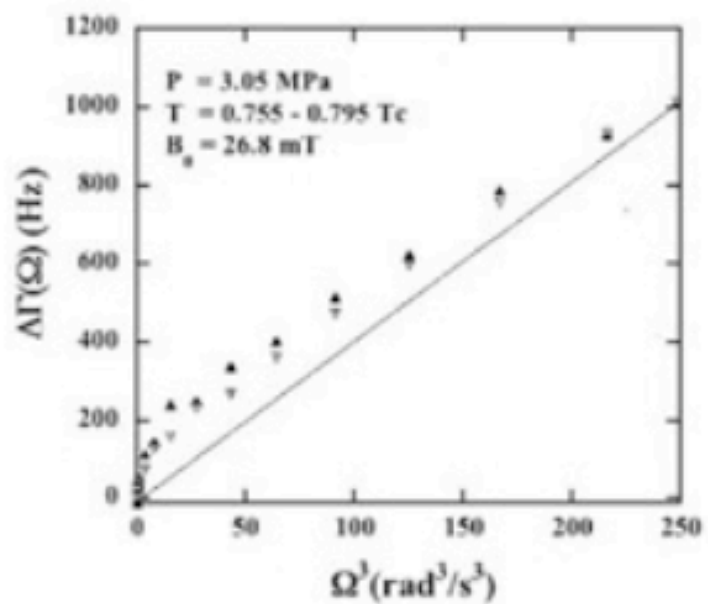
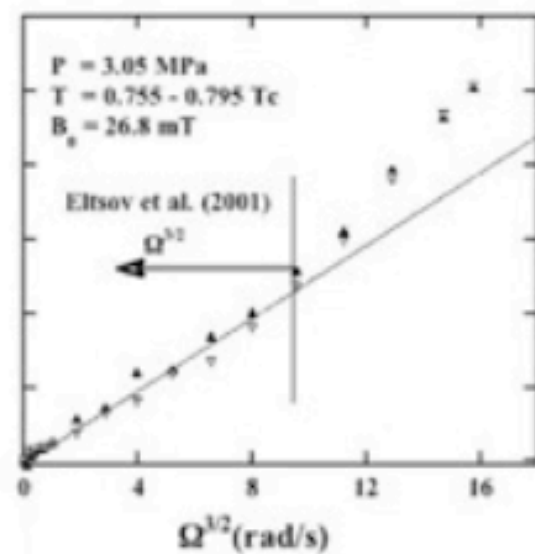
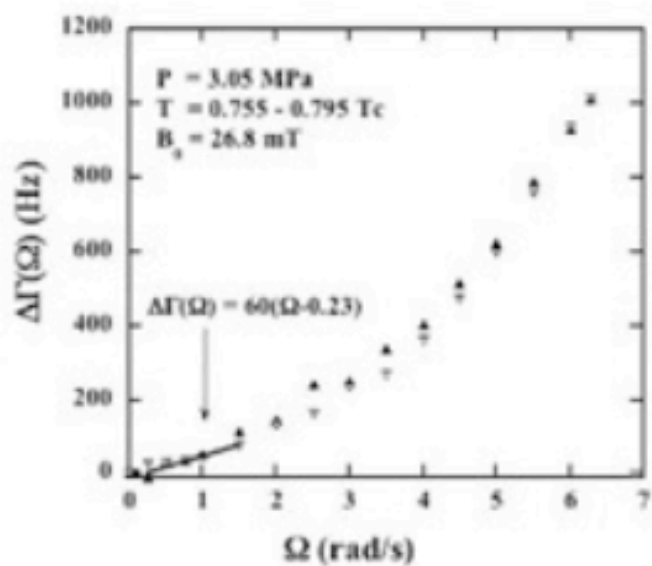


▼ τ^2 parameter

▼ τ linear parameter

τ^2 Parameter- Ω





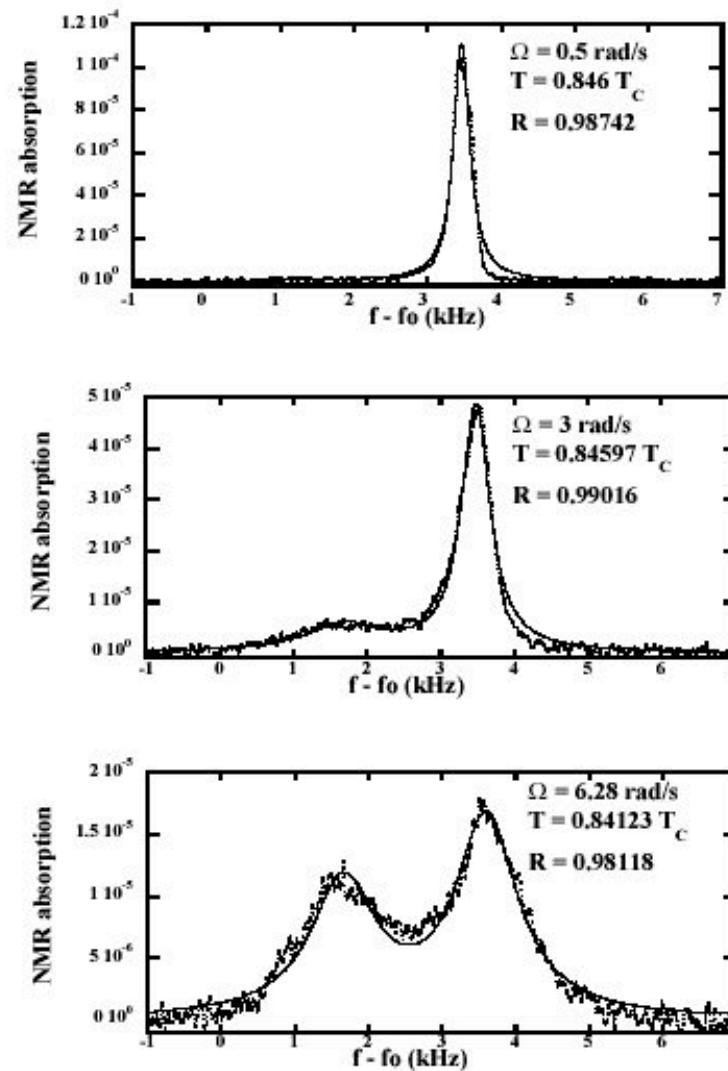


図 7.21 回転角速度の増加にともなうパルク信号の形状の変化
縦軸は核磁気共鳴吸収強度，横軸は共鳴周波数のずれ $f - f_0$ で単位は kHz.

上図は， $\Omega = 0.5 \text{ rad/s}$ ，中図は， $\Omega = 3 \text{ rad/s}$ ，下図は， $\Omega = 6.28 \text{ rad/s}$ 。
上図と中図にはローレンツ関数，下図にはダブルローレンツ関数を挿入。低回転角速度 $\Omega = 0.5 \text{ rad/s}$ では，信号の形状が非対称なので，ローレンツ関数により線幅を求めるよりも半値幅で求めた方がもっともらしいことがわかる。

Summary: Spin Dynamics and Vortex State of $^3\text{He-A}$ Studied by NMR

We have observed three distinct regions of specific line width change, $\Delta\Gamma$ with correct τ dependences, as described by Fomin and Kaminskii(1982), for the first time .

We have confirmed linear Ω dependence in $\Delta\Gamma$, as to the lower temperature Ω dependence, we observe something different from the above scenario may have in effect.